

THE PHYSICAL REVIEW

A journal of experimental and theoretical physics established by E. L. Nichols in 1893

SECOND SERIES, VOL. 120, No. 4

NOVEMBER 15, 1960

Measurements of Temperatures and Densities in Shock-Heated Hydrogen and Helium Plasmas*

WOLFGANG WIESE,[†] H. F. BERG, AND H. R. GRIEM
University of Maryland, College Park, Maryland

(Received July 5, 1960; revised manuscript received August 8, 1960)

Temperatures and densities in plasmas produced by strong magnetically driven shock waves in a "T tube" were measured spectroscopically. Local thermal equilibrium exists within the experimental accuracy for the conditions of this experiment. In both gases, the measured temperatures and densities are in disagreement with the values expected from the Rankine-Hugoniot relations, unless it is assumed that the conditions in the ambient gas are drastically affected by the initial discharge. Consistency between experiment and shock theory is achieved by considering magnetic pressure and dissociation and excitation of the ambient gas by uv radiation from the discharge.

INTRODUCTION

THE production of high-temperature dense plasmas which are in local thermal equilibrium (LTE) is of considerable interest for atomic physics and astrophysics. Plasmas in the temperature range from 10 000–100 000°K can conveniently be produced by magnetically driven shock waves in the recently developed "T tube."¹ These shock waves have a stronger attenuation than those produced in diaphragm-type tubes, and the slab of plasma behind the front is rather thin with the density decaying very fast, whereas the temperature changes much slower if ionization is not complete (heat reservoir of heat of ionization).

One approach to determine the equilibrium conditions behind the shock front would be to measure the ambient pressure and the shock velocity and to calculate the density and temperature by using the Rankine-Hugoniot relations as in work with conventional shock tubes.² A spectroscopic study with a "T tube" in helium³ showed, however, that this method can easily lead to serious errors and is of only limited value for the shock

diagnostics. It was proposed there that this is due to a significant energy transfer to the cold gas during the initial discharge by intense uv radiation, which must be considered when the conditions ahead of the shock front are formulated. As detailed calculations of this effect are very difficult, only estimates could be given, which showed that mainly the resonance lines of ionized helium would be effective, i.e., transport enough energy into a given volume ahead of the front before this was reached by the shock. Essential herein was that the mean free path of this radiation is comparable to the length of the shock tube.

The diagnostics of the helium shock wave³ was based mostly on photoelectric measurements of absolute intensities. In the experiments described here several other spectroscopic methods were used to check the consistency and applicability of the various methods and the reproducibility of the shock tube. In addition to helium, hydrogen was studied in order to eliminate any effects associated with a particular gas. If hydrogen behaved like helium the proposed mechanism for the energy transfer in helium would become more likely, because similarly to the ionized helium resonance lines the radiation of the effective Lyman-lines has a mean free path of the required order in the ambient gas. The experiments described here will also serve to give a better picture of the capabilities and limitations of the "T tube" as a thermal light source.

* Jointly supported by the Geophysics Research Directorate of the Air Force Cambridge Research Center and the Office of Naval Research.

[†] Now at the National Bureau of Standards, Washington 25, D. C.

¹ A. C. Kolb, *Phys. Rev.* **107**, 345 (1957).

² E. L. Resler, Shao-Chi Lin, and A. Kantrowitz, *Appl. Phys.* **23**, 1390 (1952).

³ E. A. McLean, E. Faneuff, A. C. Kolb, and H. R. Griem, *Phys. Fluids* **3** (November, 1960).

APPARATUS

Shock Tube

All experiments were performed with a *T*-shaped quartz tube, 2 cm in diameter and 15 cm long, which was filled to an initial pressure of 2 mm Hg with helium or to 1 mm Hg with hydrogen. Two low inductance capacitors (0.1 μ f capacity, 40-kv maximum voltage) stored the electrical energy. In order to produce high Mach number shock waves a fast discharge was required. With a circuit designed for minimum inductance a ring-frequency of 750 kc/sec could be obtained; and a discharge voltage of 35 kv provided enough energy for the shock to ionize helium almost completely and also dissociate and ionize hydrogen at the above pressures. The discharge circuit diagram is sketched in Fig. 1. A hydrogen-filled thyatron serves as a switch. As thyatrons can be used conveniently only up to voltages around 25 kv, a spark gap is put in series with it, which also damps the circuit.

Spectrograph

The shock wave spectra were observed either photographically or photoelectrically with a 3-prism Steinheil glass spectrograph. The photographic method required a shutter for extremely short exposure times to obtain space- and time-resolved pictures of the fast moving shock. To meet the particular requirements of this experiment—especially high optical transmission—a special mechanical shutter of the focal-plane type was designed.⁴ Two high-quality lenses L_1 and L_2 image the shock tube onto the slit of the spectrograph.

EXPERIMENTS

Photoelectric Intensity Measurements

Photomultipliers of the type 931A in a circuit especially designed for work with extremely short pulses were used and signals photographically recorded using fast (Tektronix 517) oscilloscopes. Extensive shielding of multipliers and cables was necessary to eliminate the noise of the discharge. The electronics and the optical system could resolve times down to 0.05 μ sec, which was sufficient for measurements of the state behind the front, because the recorded light pulses show a stationary state for several tenths of a microsecond.

The absolute intensity was measured by comparison with a carbon arc as radiation standard.⁵ The arc (Fig. 1) was imaged by a third lens L_3 into the shock tube and from there the optical path is the same as for the shock wave radiation. Losses by absorption and reflection on lens and shock tube walls were taken into account. The shock velocity was measured by imaging the shock tube on an array of slits and photoelectrically recording the arrival times of the light pulses from the shock front at these slits.

Photographic Measurements

The time-resolved photographic observation is superior to the photoelectric method insofar as the whole spectrum in spatial resolution is simultaneously shown, and the information contained in the line shapes can be utilized. Unfortunately this method is limited in its application by the insufficient sensitivity of the photographic emulsion. By using the fastest available emulsions (Kodak Royal-X and Kodak 103F) and force-developing them, satisfactory exposures of the strongest

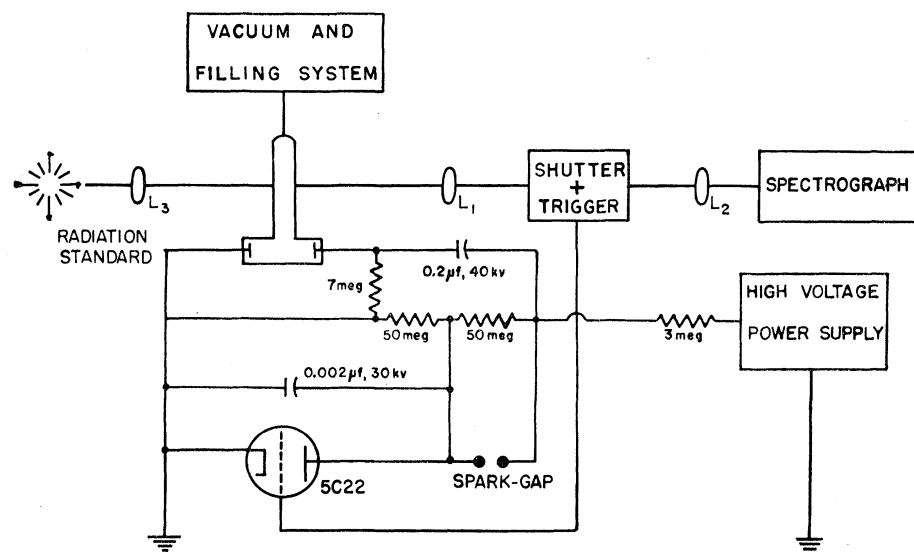


FIG. 1. Diagram of the experiment.

⁴ W. Wiese, Rev. Sci. Instr. (to be published).

⁵ J. Euler, Ann. Physik 11, 203 (1953).

spectral lines in helium and hydrogen could be obtained in 0.5 μ sec. From time-resolved photoelectric recordings zones of constant intensity ($\pm 10\%$) behind the front were measured to 0.6 μ sec for He I 5876, 0.4 μ sec for He II 4686, and 0.5 μ sec for H α . Therefore only the line profiles of He I 5876 and of H α can safely be used for the diagnostics of the stationary state behind the shock.

The films and plates were calibrated in relative intensities by means of a rhodium seven step-filter, using the carbon arc. As the exposure time for the arc had to be a factor 10^4 larger to obtain equal densities, the question arose whether the gradients of the density curves varied with exposure time. The results of several test series^{6,7} for the emulsions used show that changes in the γ value are negligible.

SPECTROSCOPIC THEORY

The intensity of a spectral line of frequency ν emitted by an optically thin layer of length l (in ergs/cm² sec steradian) is

$$J_{nm} = \frac{2\pi h \nu^3 e^2}{mc^3} \frac{g_n}{g_m} f_{mn} N_{mz} l, \quad (1)$$

where N_{mz} is the density of atoms ($z=1$) or ions ($z=2, 3, \dots$) in the upper state (labelled by m), f_{mn} the absorption oscillator strength, g_m/g_n the ratio of the statistical weights of upper and lower states of the line, and where the other symbols have the usual meaning. In case of LTE,⁸ N_{mz} is given in terms of total number density N_z of species z and partition function U_z and excitation energy E_{mz} by

$$N_{mz} = N_z \frac{g_m}{U_z} \exp(-E_{mz}/kT). \quad (2)$$

The various N_z are connected with the electron density N_e by Saha's equation

$$\frac{N_{z+1}N_e}{N_z} = \frac{2U_{z+1}}{U_z} \left(\frac{2\pi m k T}{h^2} \right)^{\frac{3}{2}} \exp(-I_z/kT), \quad (3)$$

where I_z is the ionization energy of species z .

In the partition functions

$$U_z = \sum g_m \exp(-E_{mz}/kT), \quad (4)$$

the sum is only extended to a principle quantum number n_{\max} corresponding to an excitation energy

$$E_{\max} = I_z - \Delta E = I_z - 7 \times 10^{-7} N_e^{\frac{1}{2}} \quad (5)$$

(with energies in ev), because for higher principle quan-

⁶ J. Castle and J. H. Webb, Communication No. 1581, Kodak Research Laboratories (unpublished).

⁷ J. Castle, W. Woodbury, and W. A. Shelton, Communication No. 1780, Kodak Research Laboratories (unpublished).

⁸ This assumption is consistent with an optically thin layer, if excitation and de-excitation and also ionization and recombination processes are dominated by collisions, i.e., at the high densities and intermediate temperatures of this experiment.

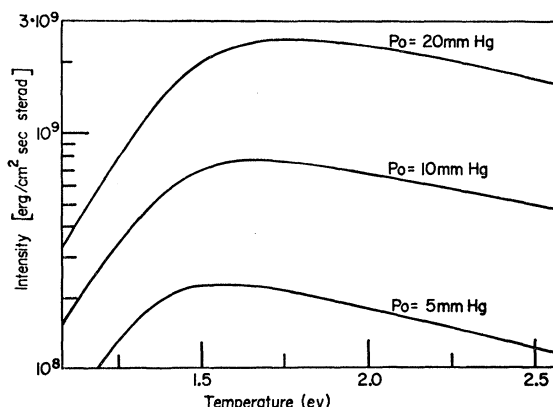


FIG. 2. Intensity of the H β line as function of temperature in a hydrogen plasma for densities corresponding to the indicated pressures of the cold gas.

tum numbers the interaction energies due to the electric micro-fields in the plasma are larger than the distance of the energy levels from the ionization limit.⁹ Likewise the excitation energy E_{\max} was used in the Saha equation instead of the ionization energy for isolated atoms or ions.

Figure 2 shows the variation of the total intensity of the H β line emitted from a pure hydrogen plasma as function of temperature for various densities $N = N_1 + N_2$ of heavy particles, using the above equations and the condition of quasi-neutrality and the ideal gas laws. A measurement of the intensity in terms of the maximum intensity for a known density can therefore serve to determine the temperature of the emitting plasma (Fowler-Milne method).

In Fig. 3 the intensity ratio of the lines He II 4686 A and He I 5876 A in a pure helium plasma is plotted as

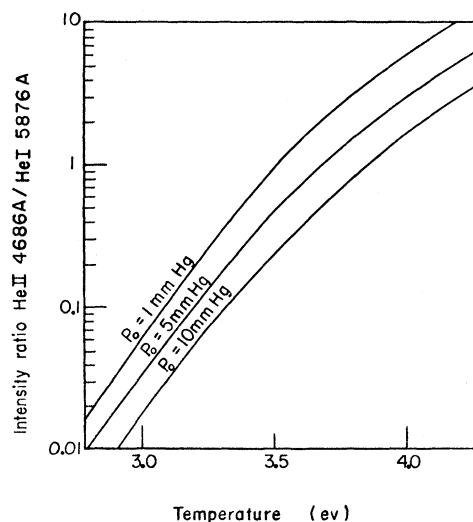


FIG. 3. Intensity ratio of the lines He II 4686 A and He I 5876 A as function of temperature in a helium plasma for densities corresponding to the indicated pressures of the cold gas.

⁹ A. Unsöld, Z. Astrophys. 24, 355 (1958).

a function of temperature, again using the above equations and assuming various values for the total density of particles, which is here $N = N_1 + N_2 + N_3$. A measurement of the relative intensities of these lines readily leads to a value for the temperature if again the density or pressure is known. (The f value for He I 5876 Å was taken from recent Hartree-Fock calculations.¹⁰) It should be noted that the shape and maximum of the intensity curve for H β and also the intensity ratio of the helium lines depend only slightly on the density, so that any reasonable assumption for the density (within a factor 2 or 3) leads to a fairly good determination of the temperature.

It is now also necessary to measure the density behind the shock front in order to make the determination of the variables complete and to test the validity of the conventional shock theory. The experimental conditions were chosen so that both gases are almost completely ionized, because then a measurement of the electron density is practically equivalent to a measurement of the total density. In case of helium N_3 was still very small whereas N_1 was already negligible.

One method for the determination of the electron density is the application of the theory of Stark broadening to measured line profiles. This method is practically independent of the temperature in the range of interest and so directly yields electron densities without assuming LTE. Here the profiles of H α and He I 5876 Å were used.

Another possibility is the measurement of the absolute continuum intensity, which is for hydrogen (with $\Delta E = I_H - E_{\max}$ again representing the advance of the continuum limit and $\Delta E_n = I_H - E_n$) given by¹¹

$$g_\nu = \frac{32\pi^2 e^6}{3\sqrt{3}c^3 (2\pi m)^{\frac{3}{2}} (kT)^{\frac{3}{2}}} \exp\left(\frac{-h\nu}{kT}\right) \times \left[\exp\left(\frac{\Delta E}{kT}\right) + \frac{2I_H}{kT} \sum_n \frac{1}{n^3} \exp\left(\frac{\Delta E_n}{kT}\right) \right] \times l, \quad (6)$$

where the sum has to be taken over all continua with lower state $E_n \leq E_{\max}$ which contribute at the frequency ν , and where the z index was omitted. It turns out that for the highly ionized plasmas encountered in these experiments the temperature dependence of g_ν is quite weak, i.e., a measurement of the continuum intensity gives a relatively accurate number for the electron density even if the temperature is only approximately known. Gaunt factors are close to 1 in this range,¹² and the H $^-$ continuum is completely negligible.

The theoretical accuracy of the formulas discussed

¹⁰ E. Treffitz, A. Schlüter, K. H. Dettmar, and K. Jörgens, Z. Astrophys. 44, 1 (1957).

¹¹ W. Finkelnburg and H. Maecker, *Handbuch der Physik*, edited by S. Flügge (Springer-Verlag, Berlin, 1956), Vol. 22, Part II.

¹² W. J. Karzas and R. Latter, Atomic Energy Commission Report AECU-3703, rev., 1958 (unpublished) and The Rand Corporation Report RM-2091-AEC, 1958 (unpublished).

in this section is of the order of 10% for the densities and better than 2% for the temperature for the conditions of the experiment. This is sufficient in view of the difficulty of achieving a similar accuracy for the measurements. The formulas for the intensities are only valid if the emission is from optically thin layers, which can easily be checked by comparing the maximum intensities with those of a blackbody at the measured temperature. All spectroscopic methods with the exception of the Stark broadening and the continuum intensity method can be used only if deviations from LTE are small, which needs to be shown experimentally or from theoretical estimates.¹¹

SHOCK EQUATIONS

The conservation equations for mass, momentum, and energy for a plane shock propagating with velocity V into a gas initially at rest are

$$N(V-u) = N_0 V, \quad (7)$$

$$NM(V-u)^2 + P = N_0 M V^2 + P_0, \quad (8)$$

$$\frac{1}{2} M (V-u)^2 + H = \frac{1}{2} M V^2 + H_0, \quad (9)$$

where $N = \sum N_z$ is the total number density of the heavy particles, i.e., the sum of the number of atoms, ions, and twice the number of molecules, M the mass of the atoms, u the flow velocity, P the pressure, and H the enthalpy per heavy particle behind the shock, and N_0, P_0, H_0 are the corresponding quantities ahead of the shock. Making use of the quasi-neutrality condition and Dalton's law one has

$$P = kT \sum_z z N_z, \quad (10)$$

and assuming complete dissociation (D =dissociation energy)

$$H = \frac{1}{N} \sum_z \left(\frac{5}{2} z k T N_z + I_z N_{z+1} \right) + \frac{1}{2} D, \quad (11)$$

where the excitation energy was neglected. The ratio of excitation and ionization energy can be estimated by using Eqs. (2), (3), and (5):

$$\begin{aligned} \frac{\sum_n N_{nz} E_{nz}}{N_{z+1} I_z} &= \frac{[\sum_n g_n E_{nz} \exp(-E_{nz}/kT)] N_z}{U_z N_{z+1} I_z} \\ &= \frac{\sum_n g_n E_{nz} \exp(-E_{nz}/kT)}{2 I_z U_{z+1} (2\pi m k T / h^2)^{\frac{3}{2}}} \frac{N_e \exp(I_z/kT)}{n_{\max}^3 N_e} \\ &\approx \frac{3 (2\pi m k T / h^2)^{\frac{3}{2}} U_{z+1}}{2 I_z U_{z+1} (2\pi m k T / h^2)^{\frac{3}{2}}}, \end{aligned}$$

with $E_{nz} \approx I_z$, $I_z - E_{nz} \ll kT$, $g_n = 2n_2$ and

$$\sum n^2 \approx \int_0^{n_{\max}} n^2 dn = \frac{1}{3} n_{\max}^3.$$

For the electron densities and temperatures in these experiments the excitation energy behind the shock

front turns out to be less than 1% of the ionization energy, and the approximation for the enthalpy is thus well justified.

If the enthalpy H_0 and the pressure P_0 are calculated for the ambient conditions, both quantities would be entirely negligible compared with H and P , respectively. But as already indicated, the enthalpy H_0 may be quite large due to trapped energy,³ and the magnetic field originating from the initial discharge may cause a magnetic pressure P_m . In contrast to the case of a shock wave propagating into an ionized gas¹³⁻¹⁵ of high conductivity there is no simple conservation law for the magnetic field here. However, it is to be expected that the magnetic pressure will be only important in front of the shock because of the diamagnetic properties of the plasma.¹⁶ With the approximation $P_0=0$ one can write, leaving P_m and H_0 as free parameters and using Eqs. (7) through (11) [in case of hydrogen half the dissociation energy D must be added on the left side of Eq. (9a), again assuming complete dissociation]:

$$N(V-u) = N_0 V, \quad (7a)$$

$$NM(V-u)^2 + kT \sum_z z N_z = N_0 M V^2 + P_m, \quad (8a)$$

$$\frac{1}{2} M(V-u)^2 + \frac{1}{2} \left[\sum_z \left(\frac{5}{2} k T z N_z + I_z N_{z+1} \right) \right] = \frac{1}{2} M V^2 + H_0 + 2(P_m/N_0). \quad (9a)$$

The first two equations can be used to determine the flow velocity u and the magnetic pressure P_m from the measured shock velocities V and spectroscopically measured temperatures and densities. The last equation then allows the calculation of the enthalpy H_0 ahead of the shock front. If the values of H_0 and P_m obtained in this way are consistent with more direct determinations, the proof would be completed that the apparent discrepancy between usual shock wave theory and spectroscopic measurements can indeed be resolved by including H_0 and P_m in the analysis.

¹³ C. S. Gardner *et al.*, *Proceedings of the Second United Nations International Conference on Peaceful Uses of Atomic Energy, Geneva, 1958* (United Nations, Geneva, 1958), Vol. 31, p. 230.

¹⁴ S. A. Colgate, *Phys. Fluids* **2**, 485 (1959).

¹⁵ A. Kantrowitz, R. M. Patrick, and H. E. Petschek, *Proceedings of the Fourth International Conference on Ionization Phenomena in Gases, Uppsala, Sweden, 1959* (North Holland Publishing Company, Amsterdam, 1960).

¹⁶ If a magnetic field exists ahead of a shock in a region of zero electrical conductivity and if behind the shock the gas is at high temperature and electrically conducting, the hot gas is not diamagnetic in the usual sense. Flux is still trapped in the shock front over a distance determined by the depth of the current layer separating the ambient field from the zero field region, i.e., over a distance of the order $mc^2\nu/(2\pi Ne^2V) \approx 0.1$ cm for an electron density $N \approx 2 \times 10^{17}$ cm⁻³, a collision frequency $\nu \approx 10^{13}$ sec⁻¹ and a shock velocity $V \approx 3 \times 10^6$ cm/sec. Since the fluid compression occurs over a distance that is smaller most of this compressed flux can "leak" out ahead of the shock. In this sense the shocked fluid is diamagnetic. But if a major fraction of the flux were trapped, the leakage would occur from a region of field $B = B_0 N/N_0$ and the enthalpy be increased by $[(N/N_0)^2 - 1] B_0^2/8\pi$. If B_0 were about 800 gauss the enthalpy discrepancy of this experiment could be explained due to ambient fields alone provided the shock compression took place over a dimension comparable to the magnetic field entrapment length. [See W. Marshall, *Proc. Roy. Soc. (London)* **A233**, 367 (1955); and Marian H. Rose, Atomic Energy Commission Report NYO 7693 (unpublished)].

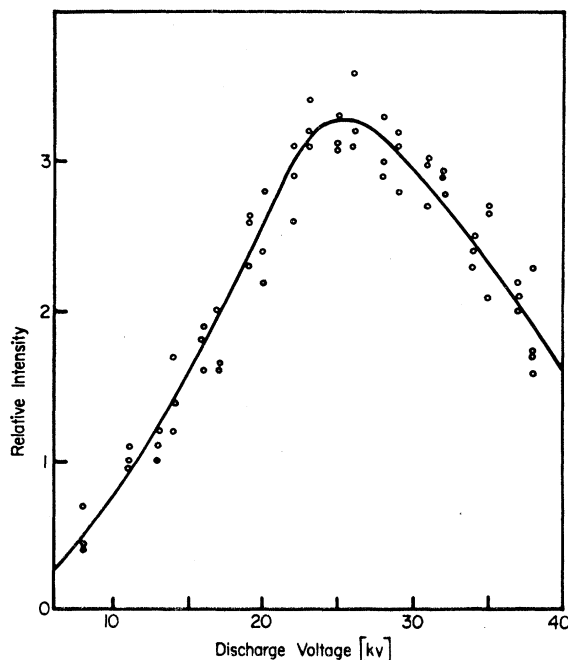


Fig. 4. Relative intensity of the H_β line as function of discharge voltage.

RESULTS

Hydrogen

The temperature was determined by applying the modified Fowler-Milne method: The relative intensity of H_β is plotted as a function of discharge voltage in Fig. 4. After estimating the density roughly, the temperature at the maximum is found by comparison with the calculated intensity function in Fig. 2, and by normalizing both curves temperature versus discharge voltage can be determined. This value for the temperature is then used in the density determination, and in an iteration process the newly found density serves to derive a better value of the temperature. Consistency is reached in a few steps.

The electron density was determined in two ways: The absolute intensity of the continuum was measured photoelectrically at 5450 Å after having checked that this wavelength region is free of impurity lines, and the profile of the H_α line was measured photographically and compared with Stark broadening theory.¹⁷ With the density and temperature so obtained a calculation of the optical thickness τ was made which yielded $\tau = 0.1$ at the line center, i.e., the emission was indeed from an optically thin layer.

Helium

The temperature was determined by measuring the intensity ratio of the lines He I 5876 Å and He II 4686 Å

¹⁷ H. R. Griem, A. C. Kolb, and K. Y. Shen, *Phys. Rev.* **116**, 4 (1959).

TABLE I. Results.

Gas	Initial pressure (mm Hg)	Shock velocity (cm/ μ sec)	Electron density (10^{17} cm $^{-3}$)		Density ratio N/N_0	Temperature (ev) T
			Line profile	Continuum		
Hydrogen	1.00 ± 0.02	5.1 ± 0.3	2.5 ± 0.5	2.0 ± 0.4	3.5 ± 0.7	2.4 ± 0.3
Helium	2.00 ± 0.03	2.5 ± 0.2	1.7 ± 0.4	...	2.6 ± 0.5	3.6 ± 0.3

photographically (see Fig. 3). A discharge voltage was selected at which these strongest lines of the spectrum were of approximately equal intensity.

The density was derived from measurements of the half-width of the He I 5876 Å line using a recently developed theory of Stark broadening for isolated lines.¹⁸ The optical thickness for both lines was found to be smaller than 0.2, i.e., again the corrections for self-absorption are small.

In Table I the mean values of the measured shock velocities, initial pressures, electron densities, and temperatures are listed. The errors are estimated from the experimental and theoretical accuracy. About 10 runs were used for the photoelectric measurements and 5 runs for the photographic measurements. Shot to shot variations are smaller than the estimated errors except for the temperature in helium.

DISCUSSION

Table II shows the calculated density ratios and temperatures as obtained from the conventional shock theory,^{19,20} using the measured velocities and initial pressures. The discrepancy between spectroscopically measured temperatures and densities and those calculated using the Rankine-Hugoniot relations with the assumption that the ambient conditions are unchanged is much larger than the experimental errors. It might be suspected that deviations from LTE are responsible for this. However, it was shown under similar conditions for helium³ that LTE was achieved within the experimental accuracy. Photoelectric observations showed furthermore that the decay behind the shock front is much slower than the rise in the front and that all spatial gradients are very small over a mean free path in the hot plasma. Also theoretical considerations indicate that LTE may be approached within a few percent for the various temperatures.¹¹

It is therefore necessary to invoke some additional pressure and enthalpy terms in the conservation equations to remove the discrepancy. The required field strengths of a few kilogauss to build up a considerable magnetic pressure are quite plausible, because the fields produced by the primary discharge at the point of observation (3 cm from the arc in case of helium, and

TABLE II. Density ratios and temperatures from conventional shock theory and enthalpies and magnetic field strengths required to achieve consistency between theory and experiment. (The errors indicated for N/N_0 and T correspond to the errors in the measurements of velocities and pressures.)

Gas	Density ratio N/N_0	Temperature (ev) T	Enthalpy (in the ambient gas) (ev)	Magnetic field (kgauss)
Hydrogen	12.7 ± 1.5	1.4 ± 0.1	15 ± 8	2 ± 2
Helium	9.0 ± 1.0	1.9 ± 0.2	25 ± 8	5 ± 2

4.5 cm in case of hydrogen) are indeed of this order. That such fields actually occur close to the shock front has also been verified experimentally. They diminish rapidly with increasing distance from the arc, and are entirely negligible at a distance of 6 cm from the arc.³

The additional enthalpies in the gas ahead of the shock front (Table II) correspond for hydrogen to almost complete dissociation and excitation and for helium to practically complete excitation. How this might be accomplished in helium by radiative energy transfer from the arc to the ambient gas has already been discussed,³ and it will now be necessary to show that a similar mechanism can be effective in hydrogen, too, in order to remove the discrepancy between spectroscopic measurement and shock theory.

One possible source of the additional energy is the Lyman line and continuum radiation from the initial discharge. As in the case of helium³ the temperature in the initial discharge will be approximately twice that in the shock-heated plasma and also the density is expected to be much higher. With a temperature of 5 ev and an electron density of 10^{18} cm $^{-3}$ the emerging uv-photon flux follows from the spectroscopic equations as $F_0 \approx 10^{24}$ photons/cm 2 sec, assuming a geometrical depth of 2 cm. (Self-absorption is negligible except for Lyman- α .) The flux reaching the region of observation (4.5 cm from the arc will be smaller by a solid angle factor of about 0.1, so that the available flux is estimated to be $F \approx 10^{23}$ photons/cm 2 sec.

The density of hydrogen molecules in the ambient gas is about 3×10^{16} cm $^{-3}$, and assuming a cross section of $\sigma \approx 10^{-17}$ cm 2 for the absorption of the uv photons it would take $t \approx (\sigma F)^{-1} \approx 1 \mu$ sec to impart an energy of about 10 ev to the molecules without too much attenuation of the photon flux. Many of the excited states are unstable, so that hydrogen atoms in the ground-state result with an average kinetic energy of about 2 ev, which will subsequently be excited by radiative energy transfer in the lines. The resulting distribution over the excited states will closely correspond to an equilibrium distribution at the source temperature,²¹ if the cores of the lines approach the blackbody limit in the discharge. This is only the case for the Lyman- α line and to a

¹⁸ H. R. Griem, M. Baranger, A. C. Kolb, and G. Oertel, (to be published).

¹⁹ E. B. Turner, Space Technology Laboratories Report TR-59-0000-00744, 1959 (unpublished).

²⁰ C. E. Faneuff, A. D. Anderson, and A. C. Kolb, Naval Research Laboratory Report NRL-5200, 1958 (unpublished).

²¹ L. M. Biberman and B. A. Veklenko, J. Exptl. Theoret. Phys. (U.S.S.R.) **37**, 164 (1959) [translation: Soviet Phys.-JETP **37**(10), 117 (1960)].

much lesser extent for Lyman- β . For higher lines the broadening in the discharge will be very large because of the Stark effect. Accordingly only the first or the first two excited states are expected to be appreciably populated, which would correspond to exciting about 40 or 70% of the atoms in the ambient gas before the shock reaches the point of observation. This also explains why, e.g., no appreciable precursor radiation at H_{β} could be observed photoelectrically.

CONCLUSIONS

The experiments have shown that magnetically driven shock waves propagating into hydrogen or helium of about 1 mm Hg pressure encounter an ambient gas which is drastically influenced by the arc producing the shock wave. Consistency between spectroscopically measured temperatures and densities and those calcu-

lated from shock theory can be achieved if radiative energy transfer from the arc to the cold gas and magnetic fields produced by the arc in the cold gas are taken into account.

Certainly not only the conservation equations will be affected but also any relaxation phenomena, which will be much less critical now than expected for a shock going into a gas at room temperature. While the influence of the radiative energy transfer on temperatures and densities will be less important for much faster shocks leading to temperatures in the million degree range it may still be of great value to overcome relaxation effects also in such experiments, and make possible the production of plasmas in LTE in magnetic shock tubes, especially in the 1–10 mm Hg pressure and 1–10 eV temperature range, which is very important for the measurement of transition probabilities and damping constants of astrophysical interest.

Dielectric Formulation of Quantum Statistics of Interacting Particles*

F. ENGLERT† AND R. BROUT

Laboratory of Atomic and Solid-State Physics and Department of Physics, Cornell University, Ithaca, New York

(Received February 25, 1960)

Formal relations between the free energy, the “dielectric constant” which expresses the response of the system to an external perturbation, and the two-particle Green’s function in temperature space are derived. Connection with perturbation expansion for free energy and for general admittance tensors are established. These results are applied to a general discussion of the random-phase approximation at finite temperature and it is shown that the sum on ring diagrams corresponds to the calculation of the dielectric constant in the approximation of the neglect of local field corrections.

I. INTRODUCTION

THE purpose of this article is twofold. In the first sections we set forth some interesting general relations connecting the dielectric constant with the two-particle Green’s function in temperature space and with the thermodynamic functions derived from quantum statistical mechanics. The reason for setting them out here is not only to make a convenient tabulation, but also to show how they may be put to use in approximate many-body theory, which brings us to the second purpose of this paper.

There are now several studies which exist on the generalization of the random-phase approximation (RPA) of the electron correlation problem to finite temperature. Since this theory gives the correct high-density limit at zero temperature and both correct high- and low-density behavior in the classical or high-temperature limit, such studies are very much in order. These theories have taken two forms:

(a) an approximate evaluation of the partition function obtained by a selection of a special class of diagrams (called ring diagrams) in analogy to Gell-Mann and Brueckner¹ and Mayer²; (b) a dynamical model for the equation of motion of the one-particle density matrix in analogy to the theory of Sawada *et al.*³ In this paper, we show directly the connection between these approaches through the abovementioned formal relations.

Section 2 recalls the definition of the dielectric functions and summarizes their formal properties, in particular the fluctuation-dissipation theorem. In Sec. 3, we express the free energy in terms of the dielectric constant. We show how to formulate RPA for the dielectric constant at finite temperature, in analogy to Nozières and Pines.⁴ When this is substituted into the

¹ M. Gell-Mann and K. A. Brueckner, *Phys. Rev.* **106**, 364 (1957).

² J. E. Mayer, *J. Chem. Phys.* **18**, 1426 (1950).

³ K. Sawada, *Phys. Rev.* **106**, 372 (1957); K. Sawada, K. A. Brueckner, W. Fukuda, and R. Brout, *Phys. Rev.* **108**, 507 (1957); R. Brout, *Phys. Rev.* **108**, 515 (1957).

⁴ P. Nozières and D. Pines, *Nuovo cimento* **9**, 470 (1958).

* This work has been supported in part by the Office of Naval Research.

† On leave of absence from Université Libre de Bruxelles, Brussels, Belgium.